PREDICTION OF METAL SORPTION IN SOILS

Westrich, H. R, Anderson, H. L., Arthur, S. E., Brady, P. V., Cygan, R. T.,
Liang, J. J., and Zhang, P. C.
Geochemistry Department
Sandia National Laboratories
Albuquerque, NM 87185-0750

N. Yee
Department of Civil Engineering and Geological Sciences
University of Notre Dame
Notre Dame, IN 46556

ABSTRACT

Radionuclide transport in soils and groundwaters is routinely calculated in performance assessment (PA) codes using simplified conceptual models for radionuclide sorption, such as the K_D approach for linear and reversible sorption. Model uncertainties are typically addressed by adding layers of conservativeness (e.g., very low K_D's), and often result in failed transport predictions or substantial increases in site cleanup costs. Realistic assessments of radionuclide transport over a wide range of environmental conditions can proceed only from accurate, mechanistic models of the sorption process. We have focused on the sorption mechanisms and partition coefficients for Cs^+, Sr^{2+} and Ba^{2+}(analogue for Ra^{2+}) onto iron oxides and clay minerals using an integrated approach that includes computer simulations, sorption/desorption measurements, and synchrotron analyses of metal sorbed substrates under geochemically realistic conditions. Sorption of Ba^{2+} and Sr^{2+} onto smectite is strong, pH-independent, and fully reversible, suggesting that cation exchange at the interlayer basal sites controls the sorption process. Sr^{2+} sorbs weakly onto goethite and quartz, and is pH-dependent. Sr^{2+} sorption onto a mixture of smectite and goethite, however, is pH- and concentration dependent. The adsorption capacity of montmorillonite is higher than that of goethite, which may be attributed to the high specific surface area and reaction site density of clays. The presence of goethite also appears to control the extent of metal desorption.

In-situ, extended X-ray absorption fine structure (EXAFS) spectroscopic measurements for montmorillonite and goethite show that the first shell around adsorbed Ba^{2+} is coordinated by 6 oxygens. The second adsorption shell, however, varies with the mineral surface coverage of adsorbed Ba^{2+} and the mineral substrate. This suggests that Ba^{2+} adsorption on mineral surfaces involves more than one mechanism and that the stability of sorbed complexes will be affected by substrate composition. Molecular modeling of Ba^{2+} sorption on goethite and Cs^+ sorption on kaolinite surfaces were performed using molecular dynamics techniques with improved Lennard-Jones interatomic potentials under periodic boundary conditions. Ba^{2+} was observed to have a preference for inner sphere sorption onto goethite, with the (101) and (110) surfaces representing the controlling sorption surfaces for bulk K_D measurements. Large-scale simulations of Cs^+ sorption on kaolinite (1000's of atoms) provide a statistical basis for the theoretical evaluation and prediction of Cs^+ K_D values. Results suggest the formation of a strong inner sphere complex

for Cs^+ on the kaolinite edge surfaces and a weakly bound outer sphere complex on the hydroxyl basal surface.

INTRODUCTION

While sorption has a great effect on absolute estimates of radionuclide transport in soils and groundwaters, current performance assessment (PA) models use simplified conceptual models for radionuclide sorption. Linear and reversible sorption (K_D approach) is rarely observed in the field because of nonlinear geochemical parameters that can significantly affect radionuclide transport mechanisms and kinetics (e.g, pH, fluid composition, ionic strength, mineral substrate structure and composition, organic complexation). Conceptual sorption model inaccuracies are typically addressed by added layers of conservativeness; that is, by the use of very low K_D's taken from default compilations of radionuclide partition coefficients (1). Not surprisingly, this approach often results in failed transport predictions, including such recent examples as vadose zone radionuclide transport of Cs at the DOE Hanford site and fracture flow transport of Pu at the Nevada Test Site. Each "surprise" decreases public confidence in the risk assessment process. We believe that realistic assessments of radionuclide transport and risk over a wide range of environmental conditions can proceed only from an accurate, mechanistic model of the sorption process. For radionuclide transport, this means that sorption models must also account for non-linearity and irreversibility.

The overall objective of our research is to provide a defensible, science-based understanding of radionuclide migration and retardation in contaminated environments. These results will provide better estimates of radionuclide movements in ground and surface waters, and will be applied to licensing and decommissioning of nuclear facilities and clean up of contaminated sites. We use complementary experimental and computational results to constrain sorption mechanisms and partition coefficients for radionuclide-soil pairs of relevance to NRC licensees at civilian nuclear facilities or decommissioned civilian nuclear facilities. We specifically rely on calculations done at the atomic level, coupled with sorption/desorption measurements that provide molecular detail, to identify and constrain the sorption process and kinetic parameters (2,3). This fine-scale detail closes the reality gap by forcing a valid sorption model into the front end of the transport calculation. Subsequent modifications that are site-specific (i.e., hydrologic fast flow paths, consideration of colloidal transport, mobilization by organic chelation, etc.) are then constrained to better reflect field observations, simply because they proceed from a realistic starting model.

Specific goals of this study include: (1) Evaluation and quantification of those critical mechanisms and geochemical parameters that control the retardation of selected divalent radionuclides on sorbing phases in near-field soils, principally clay minerals (e.g., montmorillonite) and Fe-oxides (e.g., goethite-coated sands). This work involves spectroscopic characterizations of mineral surfaces by X-ray synchrotron radiation techniques, coupled with laboratory measurements of adsorption and desorption kinetics for Sr^{2+} and Ba^{2+} (as an analogue for Ra^{2+}) on common soil minerals. Quartz is included in this study so that sorption and desorption kinetics for Sr^{2+} can be evaluated for mineral assemblages as well as for monomineralic substrates. (2) Use of atomistic computer simulations to predict radionuclide K_D values based on the partitioning of the metal cations between the solution and mineral surface. Effective bulk K_D values will be derived for the selected metals (Cs^+ and Ba^{2+}) on each of the

dominant surfaces of kaolinite clay and goethite. Calculated $K_{D's}$ are especially critical when they are lacking in the scientific literature or experimental data are wildly variable. Our theoretical treatment allows for strict *a priori* control of the chemical environment so that a consistent basis for evaluating the influence environmental variables on K_D can be obtained. Additionally, this method may help to soundly assess the distribution of experimental K_D values and potentially reduce their variance to a more meaningful and applicable level to help in the risk evaluation of a particular waste site. The ultimate goals of this work are to identify primary macroscopic features controlling radionuclide plume evolution (e.g. mineralogy, fluid flow rates, etc.) and to validate mechanistic predictions of radionuclide transport.

APPROACH

Sorption/Desorption Measurements

Batch metal sorption and desorption isotherms with individual minerals and composite mineral mixtures were measured using SWy-1, which is a reference montmorillonite clay from Wyoming, a commercial quartz (Min-U-Sil 5), which was purchased from U.S. Silica, Berkeley Springs, West Virginia, and synthetic goethite (α-FeOOH), which was prepared in our laboratory. The primary exchangeable ions on SWy-1 are Na^+ and Ca^{2+} (4), where its total cation exchange capacity is 76.4 meq/100g and its BET surface area is 31.82 m^2/g. The SWy-1 clay was rinsed three times with 1 M NaCl to saturate the basal planes with Na^+ and then rinsed with DDI H_2O to remove excess exchangeable Na^+. Min-U-Sil 5 quartz was acid washed by boiling 6 N HCl for 4 hrs to strip the grains of all surface coatings. The goethite was prepared by the addition of 200 mL of 2.5 N KOH to 50 g of $Fe(NO_3)_3 \cdot 9H_2O$ in 825 mL of DDI H_2O. The final pH of this solution was 12, after which the sample was aged for 5 days in a 60°C oven. After cooling, the supernatant was decanted and the samples were rinsed with DDI H_20 until the pH of the rinse water was constant. X-ray diffraction data verified that crystalline goethite (α-FeOOH) was synthesized. The measured BET surface area for quartz and goethite was 5.54 and 33.09 m^2/g respectively.

Sorption and desorption of Ba^{2+} and Sr^{2+} on smectite clay or goethite was measured as a function of time and pH (4-9) at 25ºC by suspending 0.1 g of the mineral powder in 100 mL of a background electrolyte solution, using a 200-250 mL polyethylene container as a batch reactor. The background electrolyte used for sorption measurements was 0.005 $CaCl_2$ or 0.001 NaCl electrolyte solutions spiked with either 1 ppm of $SrCl_2$ or $BaCl_2$. N_2 gas was bubbled through the solutions throughout the experiment to minimize carbonate levels in the slurries. After an equilibration time of 1 hour, the suspension was centrifuged and the supernatant was removed. The mineral sample was then resuspended in 100 ml of 0.005 $CaCl_2$ electrolyte. After pH adjustment, aliquots of the suspension from desorption experiments were taken once an hour over a period of up to 30 hours. For those solutions where pH was adjusted by titrating in HCl or NaOH, the suspension was sampled after pH stabilization. All aqueous sample aliquots were filtered (0.45□m) and analyzed for Ba^{2+} or Sr^{2+} by DCP-AES using matrix-matched standards. Similar experimental procedures were used for Sr^{2+} sorption and desorption experiments over a pH range of 3-10 using composite mixtures of quartz, montmorillonite and goethite.

Synchrotron Radiation Characterization

Synchrotron-based extended X-ray absorption fine structure (EXAFS) spectroscopy provides an element specific tool to probe the in-situ chemical speciation of adsorbed metals on mineral surfaces. In-situ EXAFS spectra were obtained at the National Synchrotron Light Source at Brookhaven National Laboratory with at the X-11A beamline fitted with a solid state Ge detector. Since the X-ray energy is above the Ba L-edge, the spectra are sensitive to the local coordination of sorbed Ba^{2+}, the surrounding sorbed ions, and the terminal oxygen atoms of the mineral substrate. Spectra were merged and reduced using the MacXAFS software program, which employs pre-edge subtraction, polynomial background removal, and Fourier transform routines. Non-linear least square fitting of the EXAFS data yielded quantitative information about the atoms surrounding the sorbed metal, including their coordination numbers and average bond distances. The coordination number for each type of bond was interpreted in light of known crystallographic data as well as atomistic modeling results. The phase shifts and backscattering amplitudes from either experimental results or simulation by atomistic modeling were used as references in fitting.

Computer Simulations

Large-scale molecular dynamics simulations were used to examine the sorption of Cs^{+} and Ba^{2+} from aqueous solution by the edge and basal surfaces of kaolinite and goethite, respectively. Similar interatomic potentials were developed to evaluate the interactions among the substrate and solution atoms. Partial charges were derived from molecular orbital calculations, and the Leonard-Jones parameters were parameterized from the observed structures of simple oxides, hydroxides, and oxyhydroxide phases. A flexible simple point charge (SPC) model was used to simulate the behavior of water in the system. Equilibrium structures and vibrational spectra obtained from the molecular dynamics simulation of kaolinite are in very good agreement with experimental observations (4, 5). Unique in this simulation approach is the use of a completely flexible system in which all substrate and solution atoms are allowed to freely translate during the simulation. First, we examined the sorption of Ba^{2+} onto several columnar and terminal surfaces of goethite using a molecular dynamics approach based on the new set of interatomic potentials. A comparison of the energies for inner sphere, outer sphere, and fully solvated metal complexes was made to evaluate the relative binding of Ba^{2+} on the goethite surfaces. We also completed a series of simulations for a very large periodic surface of kaolinite, incorporating several thousand atoms covering a substrate region of several thousand square Ångstroms. Eight to over a hundred Cs^{+} atoms are incorporated in the solution and allowed to equilibrate with the kaolinite substrate for simulation times up to 1 nanosecond, involving a million time steps. Analysis of the equilibrated structures provides a statistical basis for the theoretical evaluation of the Cs^{+} distribution coefficients (K_D). Previous simulations suggest the formation of a strong inner sphere complex for cesium on the kaolinite edge surfaces and a weakly bound outer sphere complex on the hydroxyl basal surface.

RESULTS

Desorption of Ba^{2+} and Sr^{2+} from SWy-1 was rapid, reaching equilibrium in less than one hour. The extent of desorption was pH-independent, reaching the same final equilibrium concentration as the sorption experiments. Metal sorption reached final values of 30 and 50%, respectively for

Ba^{2+} and Sr^{2+}. However, Sr^{2+} sorption onto both the quartz and goethite surface displayed a pH-dependent sorption trend (Fig. 1). Under acidic conditions, Sr^{2+} sorption was low, increasing with increasing pH. On the other hand, Sr^{2+} sorption onto smectite was dominantly pH-independent with a weak pH-dependent trend. The smectite surface displayed a high affinity for Sr^{2+}, sorbing over 50% of it at low pH conditions (pH~3). Two Sr^{2+} sorption experiments were conducted with composite mineral assemblages (Fig 2). The first composite mineral assemblage (CMA1) consisted of all three minerals, quartz, goethite, and smectite, in normalized quantities so as to have approximately equal surface areas for reaction. CMA1 displayed a high extent of sorption at low pH (~50% at pH 3) and sorption increased with increasing pH. The second composite mineral assemblage (CMA2) contained the same amount of quartz and goethite without the clay fraction. CMA2 exhibited low Sr^{2+} sorption at low pH, increasing significantly with increasing pH. Sr^{2+} desorption was measured for both mineral assemblages. It was found that the Sr^{2+} sorbed onto CMA1 at pH=3.8 did not fully desorb to the expected 50% level observed (sorption level for smectite at the same conditions). The desorption experiment was conducted for 30 hours and, at the end of the experiment, a small irreversibly sorbed fraction of Sr^{2+} was observed. CMA2 displayed a much higher fraction of irreversibly sorbed Sr^{2+} for desorption at a pH at 3.1, with over 40% of the total Sr^{2+} remaining sorbed onto the quartz-goethite assemblage after 30 hrs.

EXAFS results indicate that the first shell of the adsorbed Ba^{2+} on both montmorillonite and goethite surfaces consisted primarily of six (±20%) oxygen atoms. The average distance between the Ba^{2+} and first shell oxygen atom is 2.93-3.05 Å (Table 1). However, the composition of atoms in the second shell around adsorbed Ba^{2+} varies with the mineral surface coverage by the adsorbed Ba^{2+}. Si and Fe were found in the second shell of Ba^{2+} adsorbed on montmorillonite and goethite, respectively, when the pH and adsorption are low. The variation in the distances of between the adsorbed Ba^{2+} and second shell atoms also indicates the existence of element(s) other than oxygen in the shell. However, with increasing adsorption, the coordination number of Si and Fe in the second shell decreased.

Table 1. XAFS Structural Configuration of Ba^{2+} Sorbed on Montmorillonite and Goethite.

Configuration of Ba Associated with Montmorillonite				
PH	**Adsorption (mg/g)**	**Bond**	**CN**	**Distance (Å)**
3.3	15.1	Ba-O	6.9	2.73
		Ba-O	2.3	3.57
		Ba-Si	4.0	3.84
6.2	20.6	Ba-O	7.8	2.80
		Ba-Si	2.9	3.89
7.8	22.0	Ba-O	8.1	2.79
		Ba-Si	2.1	3.88
Configuration of Ba Associated with Goethite				
5.0	4.8	Ba-O	6.0	2.73
7.2	7.8	Ba-O	5.4	2.73
		Ba-Fe	1.4	3.46
9.0	10.0	Ba-O	5.0	2.79
		Ba-Fe	1.4	3.53
9.0*	1.4	Ba-O	6.1	2.60
		Ba-Fe	2.0	3.60

* Low concentration (0.001M vs. 0.005M) of $[BaNO_3]_2$ used in this test.

The simulated hydrolysis of Ba^{2+} ion, with respect to the coordination number and mean Ba-O distances, is in excellent agreement with experimental EXAFS results. Sorption with respect to both columnar (110 and 020) and terminal (101 and 021) surfaces of goethite was examined for simulation times of up to 100 ps. The periodic simulation cell consists of a goethite slab overlain by a water region containing a single solvated Ba^{2+} ion. Atoms in both the solution and the goethite slab surface were allowed to freely translate during the simulation. The goethite surface is deprotonated (to represent high pH conditions) with oxygen completing the coordination of the surface iron atoms. Significant preference for inner sphere sorption of the Ba^{2+} onto the surface was observed. The results of this study provide a consistent trend of binding energies for Ba^{2+} sorption on the various goethite surfaces (Figure 3). The terminal (101) face exhibits the strongest binding for Ba^{2+} due to the corrugated nature of the cleavage surface (Table 2). The columnar (110) surface (having 40% of the surface area) has the next largest binding energy, and probably represents the controlling sorption surface observed experimentally in bulk K_D measurements. The simulations also indicate that the columnar (020) and terminal (021) sorb Ba^{2+} weakly compared to the other common faces.

Table 2. Sorption energy of Ba atoms on goethite; inner sphere complex preferred in all cases.

	110	020	101	021
E_{total} (kcal/mol)	**Columnar**		**Terminal**	
Inner Surface	-30361 ± 8	-12368 ± 24	-8245 ± 21	-15926 ± 28
Outer Surface	-30318 ± 11	-12359 ± 25	-8110 ± 20	*-15920 ± 27
Bulk Water	-30339 ± 10	-12365 ± 26	-8113 ± 21	-15922 ± 10
$E_{sorption}$ (kcal/mol)	**-22**	**-3**	**-112**	**-4**

* Ba^{2+} migrated into the inner during the simulation

The simulations of Cs^+ sorption onto the (001) surface of kaolinite in a CsCl solution were successful in providing an equilibrated system in which a large number of sorbate metals are allowed to equilibrate with a mineral surface. Analysis of the simulation results indicates a fairly rapid equilibration of the Cs^+ onto the siloxane and hydroxyl sections of the basal (001) surfaces during the first 70 to 80 psec. The cations and chloride ions that are sorbed strongly as inner sphere complexes are fixed while the outer sphere and solvated ions maintain a dynamic equilibrium with the solvent water molecules (Figure 4). The results suggest that approximately 65% of the available Cs^+ is fixed or "retarded" by the exposed kaolinite surfaces under these conditions.

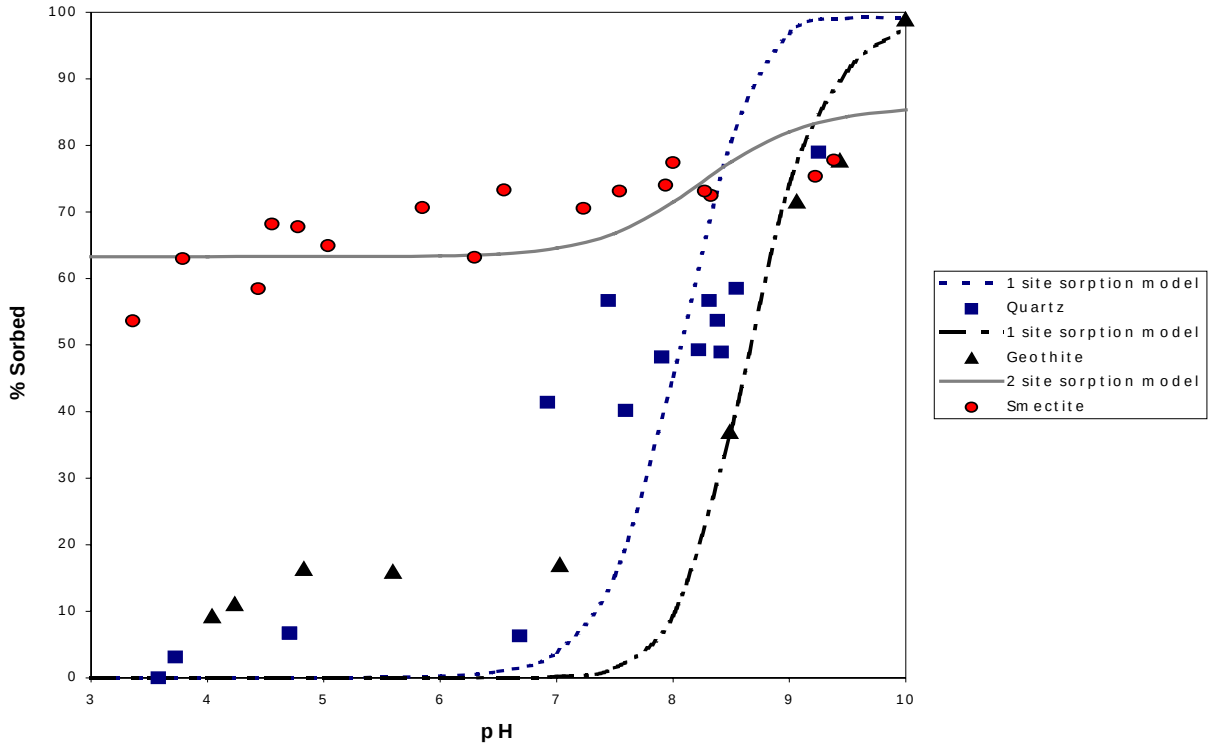

Figure 1. Effects of pH on Sr^{2+} sorption onto montmorillonite, goethite and quartz mixture.

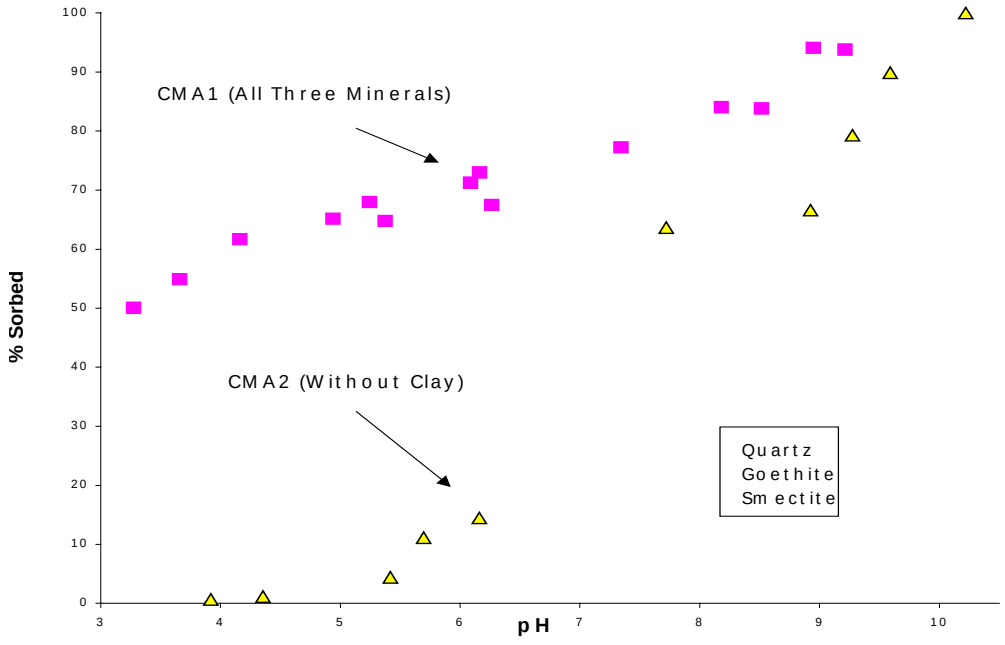

Figure 2. Effect of pH on Sr^{2+} sorption on composite mineral mixture

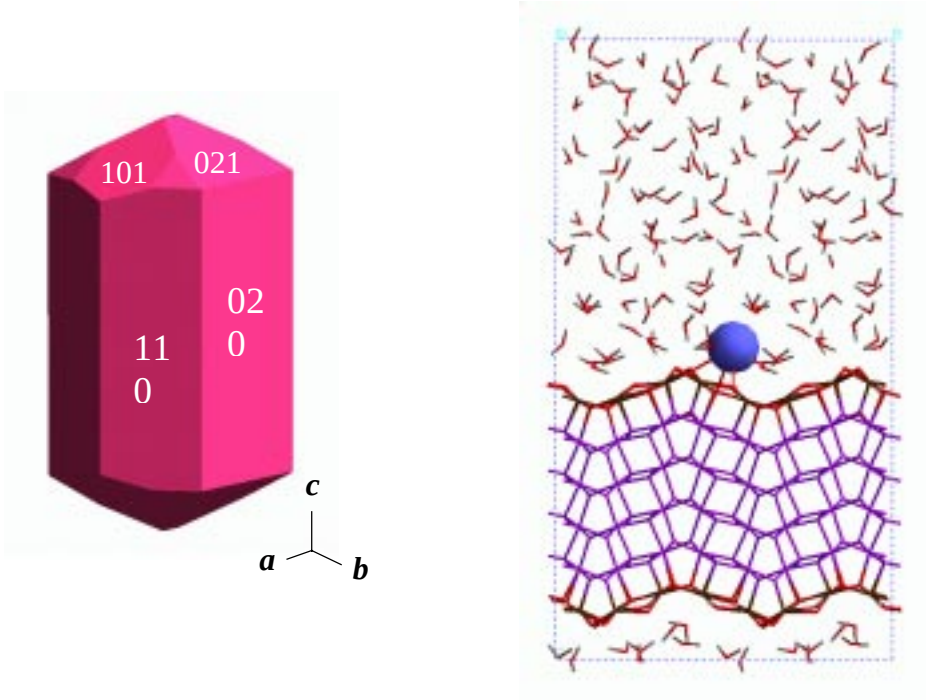

Figure 1. Ba^{2+} Adsorbed at the Inner Surface of (101) on Goethite

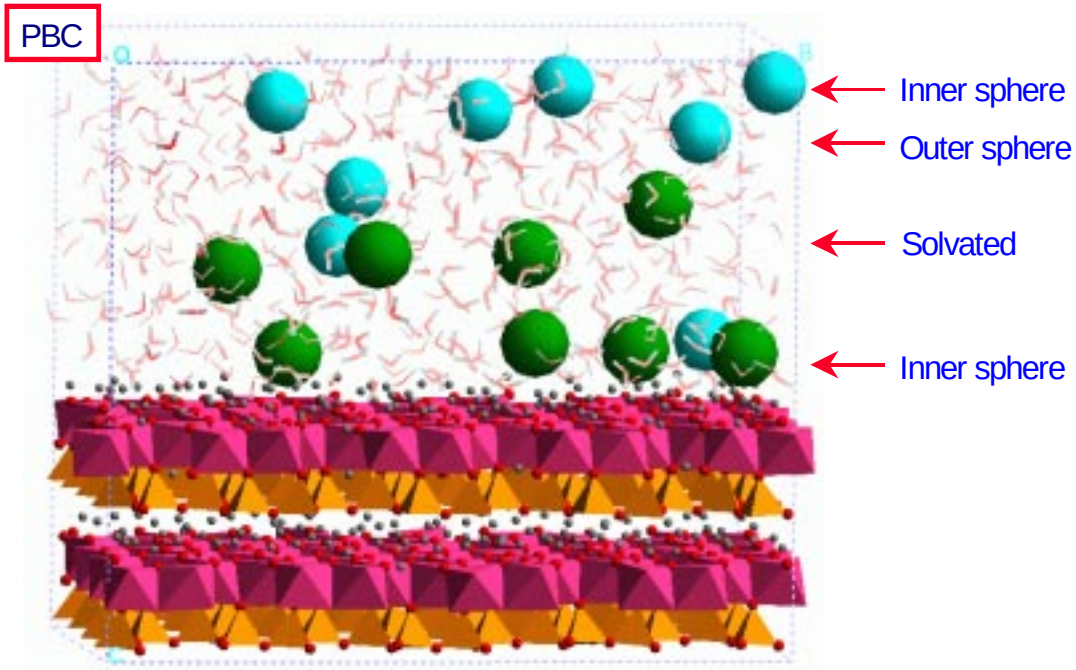

Figure 2. Simulation of Equiliberated Configuration of Kaolinite (001) Surface with CsCI Solution (Cs^{+} is light; Cl^{-} is dark)

DISCUSSION

The experimental results indicate the Sr^{2+} and Ba^{2+} sorption on montmorillonite is fully reversible and hence is an equilibrium process. The pH-independent nature of those trends suggests that the dominant sorption/desorption mechanism is cation exchange. Ba/Na exchange constants have been previous calculated (3) and are consistent with the results of this study. The adsorption isotherms for goethite and quartz indicated that Sr^{2+} sorption on these two mineral surfaces are pH-dependent and affected by the concentration of cation in the system. For the composite mineral assemblages, the Sr^{2+} adsorption capacity of montmorillonite is several times higher than that of goethite or quartz based on the mineral weight. This may be attributed to the larger specific surface area and reaction site density of montmorillonite as well as a strong cation exchange mechanism. In addition, smectite sorptive properties will dominate over that of quartz and goethite mixtures because the speciation of the surface hydroxyl sites controls the pH-dependent sorption of Sr^{2+}. Sr^{2+}, as an alkaline earth metal, forms an outer sphere complex with surface hydroxyl sites. At low pH, these sites are fully protonated and do not readily sorb Sr^{2+}. As the pH increases, the surface hydroxyl functional groups deprotonate forming a negatively charge surface site capable of sorbing positively charged aqueous cations.

Sr^{2+} sorption onto quartz and goethite can be quantified with the surface complexation model. Oxide surface speciation can be modeled with $>S\text{-}OH_2^+$, $>S\text{-}OH^0$, and $>S\text{-}O^-$ as the stoichiometries for the surface sites in contact with pure water, where >S represents a crystallographically bound metal (either Fe or Si) atom at the mineral surface. In this model, the surface acidity is described by the following protonation and deprotonation equilibria:

(Eq. 1) $$>S\text{-}OH_2^+ \Leftrightarrow >S\text{-}OH^0 + H^+$$

(Eq. 2) $$>S\text{-}OH^0 \Leftrightarrow >S\text{-}O^- + H^+$$

The corresponding mass action equations are:

(Eq. 3) $$K_1 = \frac{[>S\text{-}OH^0][H^+]}{[>S\text{-}OH_2^+]}$$

(Eq. 4) $$K_2 = \frac{[>S\text{-}O^-][H^+]}{>S\text{-}OH^0]}$$

A deprotonated surface site can sorb a Sr^{2+} ion and form a surface complex. The surface complexation reaction can be represented by the equilibrium reaction:

(Eq. 5) $$Sr^{2+} + >S\text{-}O^- \Leftrightarrow >S\text{-}O\ (Sr)^+$$

The sorption of Sr^{2+} onto the quartz and goethite can be quantified with a 1-site sorption model. The model fit curves to the sorption data are illustrated on Figure 2.

Sr^{2+} sorption onto the smectite surface can be quantified with a 2-site sorption model. Smectite is a layer aluminosilicate mineral, which displays a high affinity for aqueous cations. The metal

sorption behavior of smectite is governed by a combined effect of two types of sorption sites: 1) cation exchange sites, resulting from isomorphic substitution in the basal plane crystalline matrices, and 2) surface sites, corresponding to the silanol and aluminol co-ordination structures created along the "broken edges" of the respective Si or Al sheets. The surface complexation of Sr^{2+} at mineral edges is pH dependent, analogous to metal sorption onto oxide surfaces and can be modeled with equations 1-5. Cation exchange reactions with basal sites are pH independent due to the permanent interlayer charge. The sorption of a divalent cation Sr^{2+} onto the permanently charged basal sites can be represented as an ion exchange reaction:

(Eq. 6) $$Sr^{2+} + 2\ X\text{-}Na \Leftrightarrow 2\ Na^{+} + X_2\text{-}Sr$$

where Na^{+} is a monovalent cation located on a permanently charged basal site, X-. The corresponding mass action law is

(Eq. 7) $$K_{Sr/Na} = \frac{[Na^{+}]^2\ [X_2\text{-}M]}{[Sr^{2+}][X\text{-}Na]^2}$$

Sr^{2+} partitioning on the smectite surface can be described with a strong cation exchange site and a weak surface complexation site. The model fit to the sorption data is displayed on Figure 2.

The chemical equilibrium approach provides a thermodynamic framework where stability constants for the sorption reactions are included as part of the overall network of chemical reactions, rather than as a condition-dependent partition coefficient such as Kd. This allows for predictive calculations for a wide range of geochemical conditions without changing the values of the stability constant of the radionuclide sorption. Metal sorption onto CM1 consisted of both a pH-dependent and pH-independent component. The Sr^{2+} sorbed at low pH can be attributed to cation exchange with the smectite clay. This cation exchange reaction is pH independent. At low pH, the smectite edge sites and the hydroxyl groups on the quartz and goethite surfaces are fully protonated and do not readily from a surface complex with aqueous Sr^{2+}. As pH increases, these sites deprotonate forming a negatively charge surface hydroxyl group ($>S\text{-}O^{-}$). These surface functional groups serve as additional Sr sorption sites and the concentration of these sites is pH dependent. Since CM2 does not have a clay fraction, we do not observe a pH independent trend. We do observe a pH dependent trend, where all the Sr^{2+} sorbing onto CM2 is sorbing onto deprotonated surface hydroxyl sites. CM1 displays a small irreversibly sorbed fraction Sr^{2+}. This data set alone does not allow us to resolve which mineral surface is responsible for the irreversibly sorbed fraction. However, our observations that Sr^{2+} sorption from SWy-1 is fully reversible and the fact that CM2 results show a significantly higher extent of irreversible sorption indicates that the quartz-goethite system has a higher capacity to attenuate and immobilize strontium (via irreversible sorption). Irreversible sorption on iron oxide minerals has been documented in the literature (6). Sr^{2+} sorbed onto the mineral surface can be incorporated into the crystalline mineral structure via recrystallization, coprecipitation or solid state diffusion (7). More work is needed to constrain and quantify the desorption kinetics of Sr from iron oxide surfaces.

Synchrotron X-ray results indicate that Ba^{2+} adsorbed on mineral surface involves more than one sorption mechanism and that the stability of Ba^{2+} depends upon the extent of surface coverage.

In particular, Ba^{2+} absorbed on montmorillonite may form both inner- and outer-sphere surface complexes. At low pH (pH = 3-4), formation of $(Ba\text{-}SiO_4)_x$ complexes is possible due to dissolution of the clay, however, the complexes also may attach directly to the montmorillonite substrate. When Ba^{2+} is adsorbed on goethite, an outer-sphere surface complex forms at low pH and the inner-sphere complex forms at high pH. These results are consistent with the atomistic simulations of Ba^{2+} sorption on the various goethite surfaces. It appears that a bidentate bond may form between the goethite surface (110) oxygen and adsorbed Ba^{2+}. Therefore, the effect of adsorption of Ra^{2+} on transport of radium in subsurface should be evaluated according to the site-specific information such as mineral composition and load of Ra^{2+} on the surface.

Theoretical K_D model simulations of Cs^+ sorption onto the (001) surface of kaolinite in a CsCl solution have been successful. We have demonstrated that Cs^+ sorption on the kaolinite basal layer is characterized by two different regions of sorption. The most common sorption site for Cs^+ is that as an inner surface complex on the siloxane basal surface, while the hydroxylated gibbsite basal surface has significantly less Cs^+ sorbed. The long simulation times (200 psec) for the molecular dynamics runs provide ample time for relaxation of the solution components in order to achieve an equilibrated environment. Comparison of sorbed site concentrations with the solvated Cs^+ for the equilibrated systems provides a statistical means of obtaining K_D and retardation factors. Our modeling results for the basal surface of kaolinite indicate realistic values for metal sorption (63% sorbed) for the particular set of environmental conditions. Also, smaller scale simulations of the Cs^+-kaolinite interface suggest a difference in sorption behavior on the basal and edge surfaces. The strongest binding sites for Cs^+ sorption, based on these molecular dynamics simulations, occur on the cleavage edge sites on the (100), (010), and (110) family of surfaces. The next steps in our theoretical modeling efforts include scaling the atomistic simulation results to field applications, where more appropriate solution concentrations and compositions are needed as input parameters.

ACKNOWLEDGEMENTS

This research was supported by the U.S. Nuclear Regulatory Commission/Division of Research/Waste Management Branch and the U.S. Department of Energy under contract DE-AC04-94AL85000 to Sandia National Laboratories.

REFRENCES

1. W. E. Kennedy, Jr., and D. L. Strenge, Residual radioactive contamination from decommissioning: Technical basis for translating contamination levels to annual total effective dose equivalents. NUREG/CR-5512, Vol. 1, U.S. Nuclear Regulatory Commission, Washington, DC, (1992).
2. Brady, P. V., Cygan, R. T., and Nagy, K. L., Molecular controls on kaolinite surface charge. **Journal of Colloid and Interface Science**, 183, 356-364, (1996).
3. Westrich, H. R., Brady, P. V., Cygan, R. T., Gruenhagen, S. E., Anderson, H. L., and Nagy, K. L. Characterization of retardation mechanisms in soil. **U.S. Nuclear Regulatory Commission Report**, NUREG/CR-6603 and SAND98-0419, 23 pp., (1998).

4. Cygan, R. T., Nagy, K. L., and Brady, P. V., Molecular models of cesium sorption on kaolinite. In E. A. Jenne, Ed., **Adsorption of Metals by Geomedia**, Academic Press, San Diego, 383-399, (1998).
5. Hobbs, D., Cygan, R.T., Nagy, K. L., Schultz, P.A. and Sears, M. P., Full *ab initio* Optimization. All-Atom Ab Initio Energy Minimization of the Kaolinite Crystal Structure. **American Mineralogist**, 82, 657-662, (1997).
6. Axe, L., and Anderson, P. R., Sr diffusion and reaction within Fe oxides: Evaluation of the rate-limiting mechanism for sorption. **Journal of Colloid and Interface Science**, 175, 157-165, (1995).
7. Brady, P. V., Brady, M. V., and Borns, D. J., **Natural Attenuation of Hazardous Waste: CERCLA, RBCAs, and the Future of Environmental Remediation**, CRC Press, 245 p, (1997).